Available online at www.sciencedirect.com

SciVerse ScienceDirect

Ceramics International 38 (2012) 2243–2251

CERAMICS INTERNATIONAL

www.elsevier.com/locate/ceramint

Fundamentals and applications on *in situ* spinel formation mechanisms in Al_2O_3–MgO refractory castables

E.Y. Sako [a,*], M.A.L. Braulio [a], E. Zinngrebe [b], S.R. van der Laan [b], V.C. Pandolfelli [a]

[a] *Federal University of São Carlos, Materials Engineering Department, São Carlos, SP, 13656-905, Brazil (FIRE Associate Laboratory)*

[b] *Tata Steel Europe – Ceramics Research Centre, IJmuiden, The Netherlands*

Received 11 August 2011; received in revised form 21 October 2011; accepted 31 October 2011

Available online 4 November 2011

Abstract

Although the physical expansion associated with the *in situ* formation of magnesium–aluminate spinel ($MgAl_2O_4$) is well-reported, some questions related to this behavior, such as the different volume change values experimentally attained when compared to theoretical one and the pore generation after the reaction, remain open. Thus, the main objective of this work is to shed some light on these questions by evaluating a cement-bonded alumina–magnesia castables, designed using dead-burnt magnesia of different particle size ranges. Microstructural observations suggested that the faster Mg^{2+} migration during the spinel formation led to vacancy accumulation and, consequently, to pore generation, as a direct result of the Kirkendall effect. Additionally, the overall expansion of alumina–magnesia castables seemed to be ruled by two main factors: its sintering efficiency and the different possibilities of the Al_2O_3 and MgO interactions in the mixture. Those consequences, however, do not usually affect the castable corrosion behavior in industrial applications, due to the benefits imposed by the structural constraint.

Keywords: B. Microstructure; C. Diffusion; D. Spinel castables

1. Introduction

Wagner, Carter, Navias and many other authors [1–6] placed great efforts on the investigation related to magnesium aluminate spinel formation mechanisms. Their results pointed out that the reaction was controlled by an inter-diffusion mechanism of Al^{3+} and Mg^{2+} ions through a fixed oxygen lattice (O^{2-} was considered immobile due to its higher ionic radius and, consequently, lower diffusivity). Therefore, Al^{3+} would migrate from the alumina particles to the magnesia ones and Mg^{2+} would diffuse in the opposite direction, leading to the spinel (MA) layer formation at the interface between the alumina and magnesia particles, according to the illustration in Fig. 1. Due to the reactants reaction, this layer would then grow and push the surrounding structure as the total spinel formed would result in a higher final volume than the one where Al_2O_3 and MgO were originally located. This displacement is due to the volume change associated with the compounds density difference and, considering the stoichiometric proportions (1:1 molar ratio or 72 Al_2O_3:28 MgO mass ratio), it can be calculated as:

$$\frac{1}{\rho} = \frac{Al_2O_3\ wt\%}{\rho\ Al_2O_3} + \frac{MgO\ wt\%}{\rho\, MgO} = \frac{0.72}{3.99} + \frac{0.28}{3.58} \rightarrow \rho = 3.87\ g/cm^3 \quad (1)$$

As the spinel density is 3.58 g/cm^3, the density difference leads to an intrinsic volumetric expansion close to 8.1%, according to the following:

$$\Delta V = \frac{3.87}{3.58} \sim 8.1\% \quad (2)$$

In these studies, there were also attempts to explain the spinel expansion values experimentally attained, which were always higher than the theoretical value above-calculated. According to Wagner's mechanism [1], the ions inter-diffusion for the spinel reaction must keep the system electroneutrality. Thus, for the diffusion of each two Al^{3+} ions toward the magnesia side, three Mg^{2+} ions should migrate in the opposite

* Corresponding author.

E-mail addresses: eric.ysako@gmail.com (E.Y. Sako), vicpando@ufscar.br (V.C. Pandolfelli).

0272-8842/$36.00
doi:10.1016/j.ceramint.2011.10.074

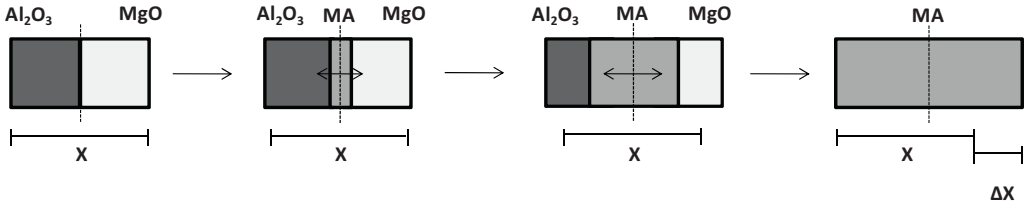

Fig. 1. Spinel formation process based on a simultaneous diffusion of Mg^{2+} and Al^{3+} through an oxygen lattice. The reaction is followed by a volumetric expansion [2].

direction, resulting in a higher content of spinel at the alumina side. Wagner's mechanism is schematically presented in Fig. 2.

Considering the compounds molar volume (MgO: 11.25 cm^3, Al_2O_3: 25.56 cm^3 and $MgAl_2O_4$: 39.77 cm^3), the reaction at the magnesia side ($4MgO \rightarrow MgAl_2O_4$) results in volume shrinkage and does not account for the system overall expansion. Therefore, Wagner stated that the permanent volumetric change associated with the spinel generation would be fully related to expansion of the alumina portion. As observed in Fig. 2, four Al_2O_3 mols change into three $MgAl_2O_4$ mols, resulting in $\Delta V \sim 16.7\%$, which is much higher than the value commonly reported ($\Delta V \sim 8.1\%$).

Based on those previous studies, Nakagawa [7] found out later that even Wagner's mechanism was not definitive and different expansion values could still be attained, according to the R parameter, which represents the spinel thickness ratio and expresses the amount of spinel formed at the alumina side (for the Wagner's mechanism, for example, $R = 3$, as the spinel layer is three times thicker at the alumina side). Nakagawa identified many factors which could affect R and consequently the overall expansion, such as the solid solubility of alumina at high temperatures, the purity of the magnesia and alumina particles, the number of contacts, the diffusion of MgO vapor and also the higher Mg^{2+} mobility in the oxygen lattice. According to this author, for the extreme situation when $R = \infty$, the reaction is conducted by an unidirectional flux of Mg^{2+} ions and the ΔV value can reach 56%.

Moreover, besides affecting the spinel volumetric expansion, the R increase seems also to induce the Kirkendall effect, which was first reported by Smigelskas and Kirkendall in 1947 [8]. This effect takes place when the inter-diffusion of one of the diffusing species is much faster than the other, leading to the formation of a pore in the initial location of the lower mobility component. When magnesium aluminate spinel is formed via solid state reaction with a high R factor value, the Mg^{2+} unidirectional diffusion is favored. The consequence is the counter-flux of vacancies which accumulate where MgO was initially placed, resulting in the Kirkendall porosity.

Fan et al. [9] recently published an interesting paper about the production of zinc aluminate spinel nanotubes based on the Kirkendall effect. These authors used a nanometric ZnO wire coated by a uniform layer of Al_2O_3 and, after the thermal treatment, the $ZnAl_2O_4$ nanotube was formed by the Zn^{2+} diffusion to the external alumina layer. Fig. 3 shows the nanotube fabrication process. Although zinc aluminate was the example used in the work, the authors confirmed that this is a common reaction in the production of other sorts of spinel, such as magnesium aluminate ($MgAl_2O_4$).

Modelings and equations have been developed in order to calculate the cations and vacancy flux, as well as the fraction of generated and/or annihilated vacancies in the reactions involving the Kirkendall effect [10–12]. However, only one of them [12] aimed to calculate the volumetric change associated with the pore formation, applying complex computing simulations based on specific boundary conditions. Moreover, none of the investigations were related to refractory compositions and, as a consequence, no report of the Kirkendall effect in spinel refractory castables has been released. Therefore, some

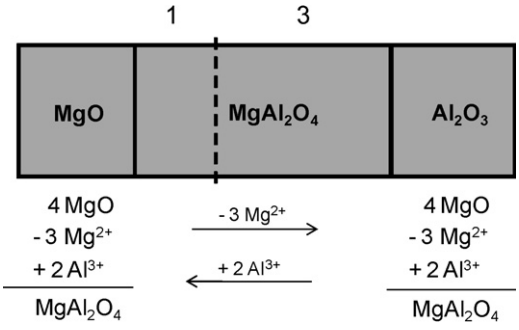

Fig. 2. Spinel formation according to Wagner's mechanism. The dashed line indicates the original alumina–magnesia interface [1].

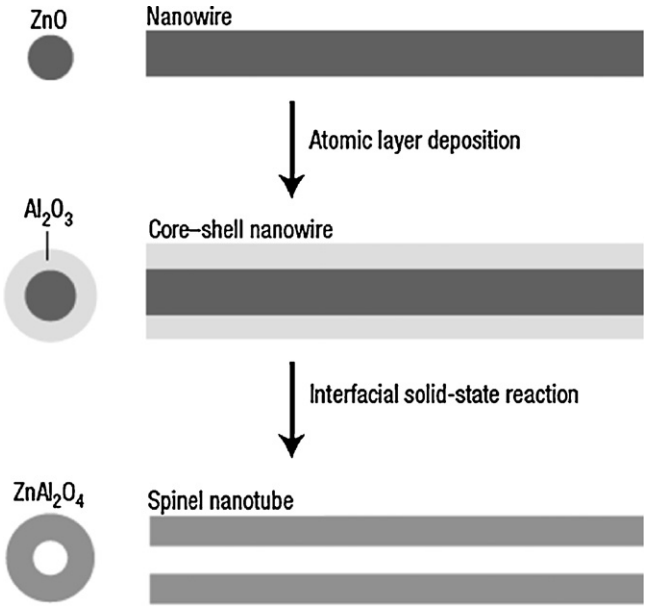

Fig. 3. $ZnAl_2O_4$ nanotube fabrication based on the Kirkendall effect [9].

questions related to the expansive behavior of these materials remain open.

A suitable example is the effect of magnesia grain size on the overall expansion of *in situ* spinel-forming castables. Braulio et al. [13] investigated this aspect and concluded that the addition of coarser magnesia grains led to higher values of residual expansion. However, considering that the same magnesia volume was used, regardless of the magnesia grain size, different values of overall expansion would not be expected. The behavior observed by Braulio et al. [13] was also previously detected in other studies involving expansive reactions, such as the magnesia hydration [14] or the silicon carbide oxidation [15]. In these cases, the use of coarse raw-materials also resulted in greater volumetric change and even cracks due to the generated stress.

Another relevant question is associated with the corrosion resistance of spinel refractory castables. Even presenting an expansive reaction which most likely leads to pore formation, castables containing *in situ* spinel usually present excellent performance in industrial units [16,17]. Braulio et al. [18] and Sako et al. [19] stated that chemical and microstructural aspects, such as the calcium aluminate phase distribution in the matrix, imparted an important role in the castable slag resistance. The mechanism proposed by these authors was appropriate for the evaluated testing conditions, but it did not consider several other variables, such as the magnesia grain size. Thus, the relationship between the corrosion resistance and the spinel formation mechanism is not yet fully understood.

Considering this scenario, the objective of the present work is to analyze indirect evidence of the Kirkendall effect and shed some light on three open questions:

- Is the spinel formation reaction ruled by the Kirkendall effect in spinel-forming refractory castables?
- What is the relationship between the castable overall expansion and the magnesia grain size?
- If the *in situ* spinel formation is followed by expansion and pore generation, why do spinel-forming castables present excellent corrosion resistance in industrial applications?

2. Experimental procedure

Three vibratable alumina–magnesia castables (M1, M2 and M3) were designed using dead-burnt MgO of different grain sizes (95 wt% MgO, C/S = 0.37, Magnesita Refratários S.A., Brazil): $D_{max} < 13$, <45 and <100 μm. As shown in Table 1, for all of them tabular alumina ($D_{max} \leq 6$ mm, Almatis, Germany) was used as the refractory aggregates and calcium aluminate cement (Secar 71, Kerneos, USA) as the binder agent. The castables matrix also comprised fine tabular alumina ($D_{max} < 200$ μm, Almatis, Germany), reactive alumina (CL 370, $D_{max} < 10$ μm, Almatis, Germany) and microsilica (971 U, Elkem, Norway). The magnesia and fine alumina contents were selected considering a potential total spinel formation after the thermal treatment equal to 21 wt% for all castables.

Table 1
Differences among the distinct castables' compositions. All of them comprised also 62 wt% of coarse tabular alumina, 6 wt% of CAC and 1 wt% of microsilica.

Raw materials	Content (wt%)			
	M1	M2	M3	PF
Tabular alumina ($d < 200$ μm)	18	18	18	10
Reactive alumina CL 370	7	7	7	–
Dead-burnt MgO ($d < 13$ μm)	6	–	–	–
Dead-burnt MgO ($d < 45$ μm)	–	6	–	–
Dead-burnt MgO ($d < 100$ μm)	–	–	6	–
Pre-formed spinel AR78 ($d < 0.5$ mm)	–			21

The castables' preparation followed the same procedure described by Sako et al. [20]. The water content required for suitable casting varied from 4.0 to 4.2 wt%, providing good workability regardless of the MgO grain size. In order to evaluate whether the Kirkendall effect rules the spinel formation, scanning electron microscopy (SEM) images of the castables microstructure after firing at different temperatures (1000, 1150, 1300 and 1500 °C) were attained (JEOL JSM-5900 lV, The Netherlands). Based on these images, pore size distribution measurements were conducted using the Noran NSS 2.2 analyzer software (Thermo Fisher Scientific, Madison, USA).

The castable's expansive behavior was also analyzed by the assisted sintering technique. The tests were carried out in refractoriness-under-load equipment (Model RUL 421E, Netzsch, Germany), where the dimensional linear change was measured as the sample was heated up to 1500 °C (3 °C/min), followed by a dwell time of 5 h at this temperature and under a compressive load of 0.02 MPa.

Samples were also produced into a cylindrical shape (50 mm × 50 mm) with a 20 mm diameter × 25 mm depth internal hole for the slag attack experiments. After previous firing at 1500 °C for 5 h, the samples' hole was filled with 10 g of industrial slag (Table 2) and then heated up again to 1500 °C for 2 h in a vertical tube furnace (HTRV 100-250/18 GERO, Germany) in air in order to perform the tests.

Aiming to evaluate the effects of the castable expansion level on the corrosion resistance, slag attack experiments were also conducted under constraint. Firstly, a high-strength alumina brick was prepared with a 55 mm diameter internal hole in order to provide the desired constraint. After pre-firing the material, a cylindrical sample as the one described above was molded inside the brick hole. The whole set was pre-fired at 600 °C for 5 h and the corrosion experiment was then conducted according to the above-reported procedure.

Table 2
Chemical composition (wt%) of the steel ladle industrial slags used for the corrosion tests.

MgO	Al_2O_3	SiO_2	CaO	MnO	Fe_2O_3
8.8	1.7	7.5	34.2	3.6	43.6

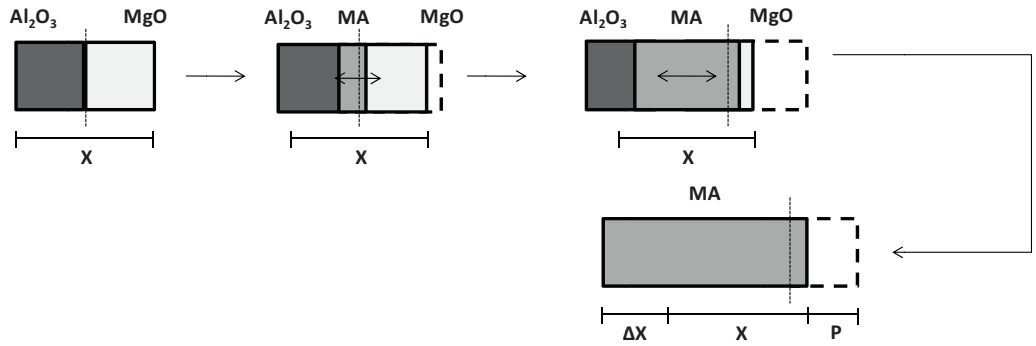

Fig. 4. Spinel formation process with high thickness ratio, generating the Kirkendall porosity.

3. Results and discussion

3.1. Is the spinel formation reaction ruled by the Kirkendall effect in spinel-forming refractory castables?

According to the aspects described above, the faster Mg^{2+} ions diffusion and the likelihood of spinel formation with high thickness ratio, favor the one-direction flux of magnesium ions and, consequently, the vacancies concentration, generating the Kirkendall porosity. Based on these features, an optimized description of the spinel formation is suggested in this work and schematically presented in Fig. 4. The $MgAl_2O_4$ formation would be firstly carried out at the particles interface, occupying, however, mostly the alumina portion. The MA layer then grows and a local volumetric change (ΔX) is detected. Nonetheless, due to the greater share of spinel formed at the alumina side (high R value), ΔX is higher than the intrinsic theoretical value of 8.1%. In addition, the Kirkendall porosity contribution (P) to the overall expansion should also be considered. In cases in which $R = \infty$, the P value would represent the MgO original volume.

In alumina–magnesia refractory castables, the spinel formation ruled by the Kirkendall effect should lead to an increase in the average pore size as the magnesia grains are gradually consumed. In order to check if this effect takes place in practice for cement-bonded *in situ* spinel-containing castables, SEM images of the M2 composition (containing MgO < 45 μm) were attained at different sintering temperatures (Fig. 5) and the pore size distribution in each stage was measured (Fig. 6).

The average pore size (d50) for the castable M2 fired at 1000 °C was close to 5 μm and this value barely changed when the firing temperature increased up to 1150 °C. According to Zhang and Lee [21], the spinel formation usually takes place at temperatures above 1150 °C and, therefore, no expansion or pore generation associated with this reaction would be expected

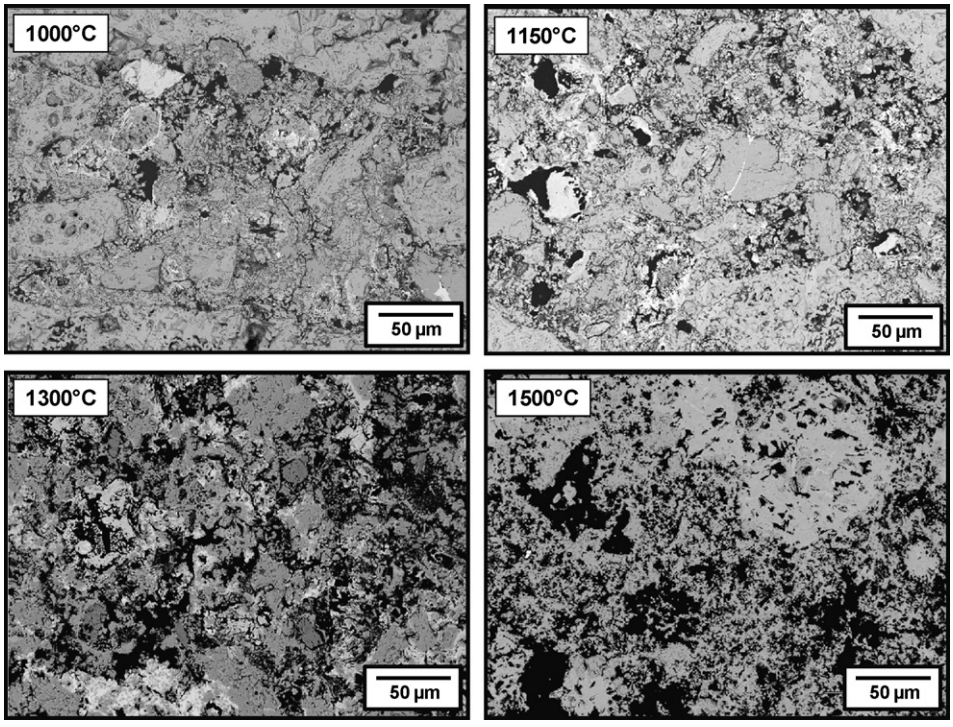

Fig. 5. Micrographs of the sample containing MgO < 45 μm (M2) after firing at different temperatures (1000, 1150, 1300 and 1500 °C) for 5 h.

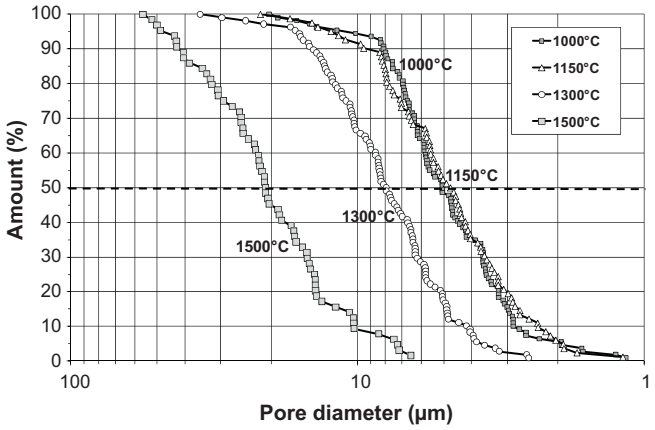

Fig. 6. Pore size distribution of sample containing MgO < 45 μm (M2) fired at different temperatures (1000, 1150, 1300 and 1500 °C) for 5 h. The dotted line indicates the average pore size (d50).

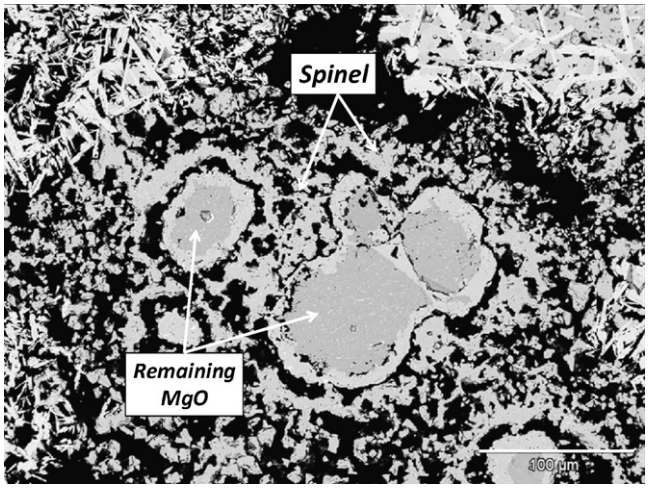

Fig. 8. Microstructure of M3 (MgO < 100 μm) sample after firing at 1500 °C for 5 h, highlighting the remaining magnesia particles.

at lower temperatures. Additionally, although some authors [22–24] stated that calcium dialuminate (CA_2) is generated at this temperature range in cement-bonded castables, leading to a small residual expansion, no significant effects on the castable porosity profile has been reported, most likely due to the presence of microsilica in this system [23].

When the sample was thermally treated at 1300 °C and 1500 °C, an increase in the d50 value was detected (8 and 22 μm, respectively), which is relevant and indirect evidence of the Kirkendall effect associated with the spinel formation. This feature presented in Figs. 5 and 6 also matches with the results attained by Braulio et al. [13]. According to these authors, most of the expansion measured for the alumina–magnesia castable containing this MgO source was detected between 1300 °C and 1500 °C, which was the temperature range of higher pore size change detected in this work.

Besides this, another aspect which would reinforce the Kirkendall effect in alumina–magnesia castables is the relationship between the average pore size after the spinel reaction and the magnesia grain size used. Aiming to evaluate this aspect, Fig. 7 shows the pore size distribution of samples M1 and M2 after firing at 1500 °C for 5 h. The results for the M3 sample (MgO < 100 μm) was not included due to the presence of remaining MgO grains in many regions of the microstructure even after the thermal treatment at 1500 °C (Fig. 8), which makes the correlation between the castable pore size and the MgO particle size difficult.

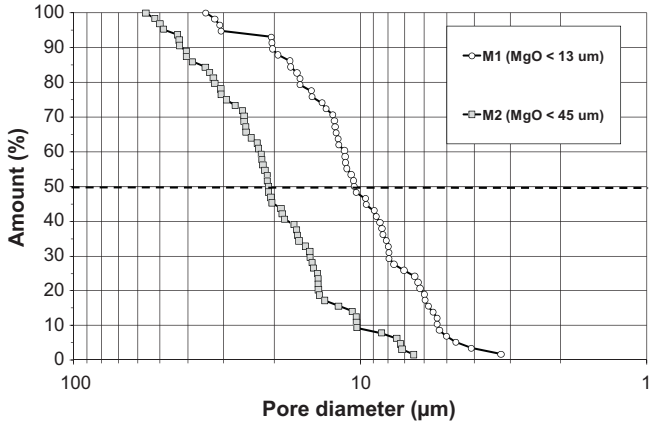

Fig. 7. Pore size distribution of samples M1 and M2 after firing at 1500 °C for 5 h. The dotted line indicates the average pore size (d50).

In Fig. 7, the difference in the pore size distribution is clear: d50 of the M2 sample is close to 22 μm, whereas it is 11 μm for M1. These results indicated that castables containing coarser MgO grains would also present a higher amount of larger pores, suggesting a relationship between the pore diameter and the magnesia grain size. This relationship was confirmed in Fig. 9, which shows micrographs of the castables containing different MgO grain sizes (M1, M2 and M3) after firing at 1500 °C for 5 h. In these images, larger pores were detected in the microstructure of M3 sample, smaller ones in the M1 micrograph, whereas M2 presented an intermediate pore profile. Moreover, the presence of spinel rims around those pores also highlights that they were previously occupied by MgO particles and, therefore, the Kirkendall effect ruled the spinel formation in these castables by the preferential out-flux of Mg^{2+} toward the surrounding alumina.

3.2. What is the relationship between the castable overall expansion and the magnesia grain size?

Although the Kirkendall effect seems to be the actual reason for the pore formation in spinel-forming castables, it does not explain the different expansion values measured when distinct magnesia grain sizes are used. Fig. 10 shows the thermal expansion profile up to 1500 °C of M1, M2 and M3, highlighting the increasing overall expansion as a function of the MgO granulometry [25]. Considering that the same volume of dead-burnt magnesia was added to the three castables, the total pore volume generated after the spinel reaction should also be the same regardless of the MgO average grain size.

Although the reaction for the M3 sample involves a higher local reaction volume and, therefore, the expansion level and

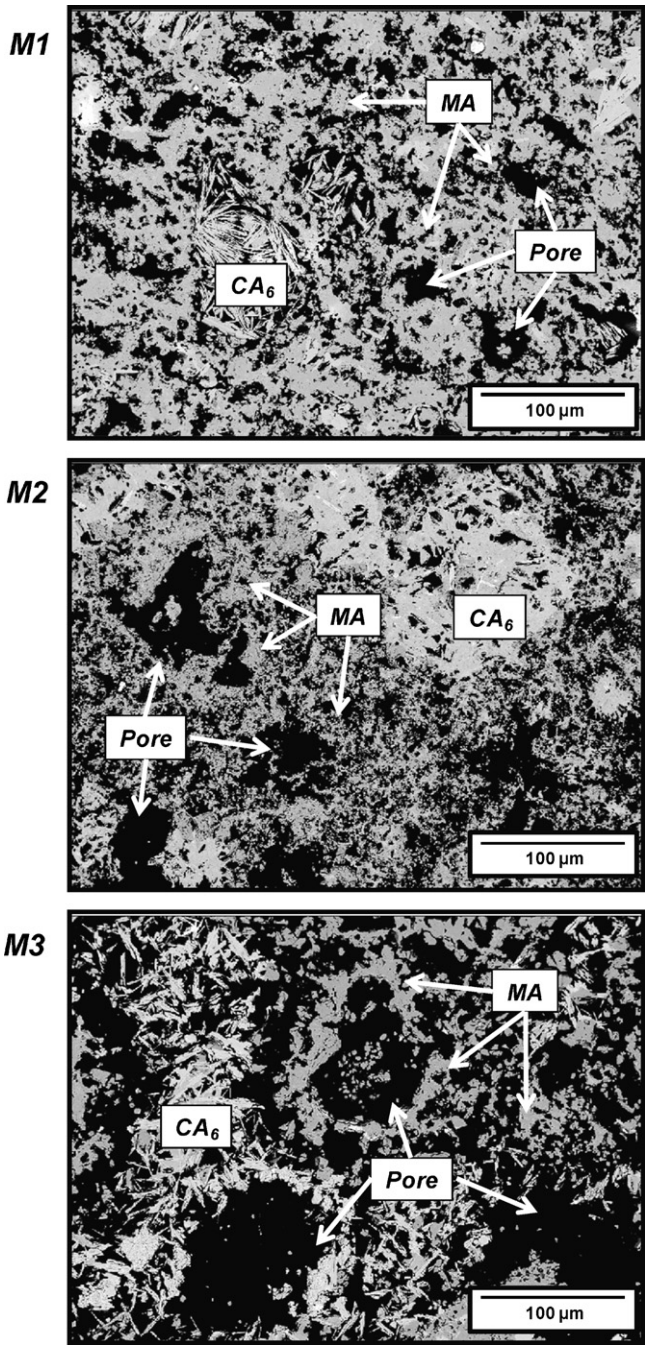

Fig. 9. Microstructure of the castables M1 (MgO < 13 μm), M2 (MgO < 45 μm) and M3 (MgO <100 μm) after firing at 1500 °C for 5 h.

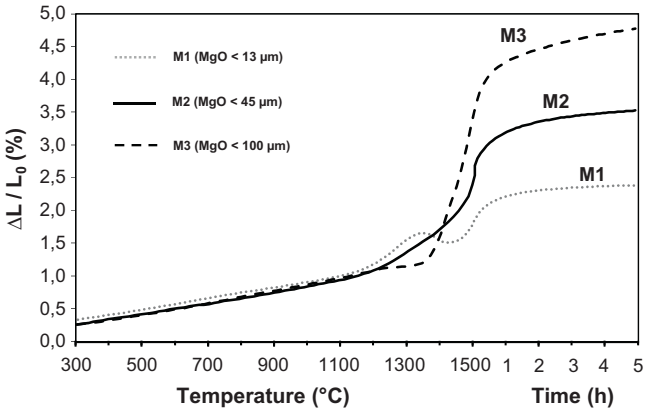

Fig. 10. Expansive behavior of alumina–magnesia castables containing MgO of different grain sizes up to 1500 °C with a dwell time of 5 h at this temperature [25].

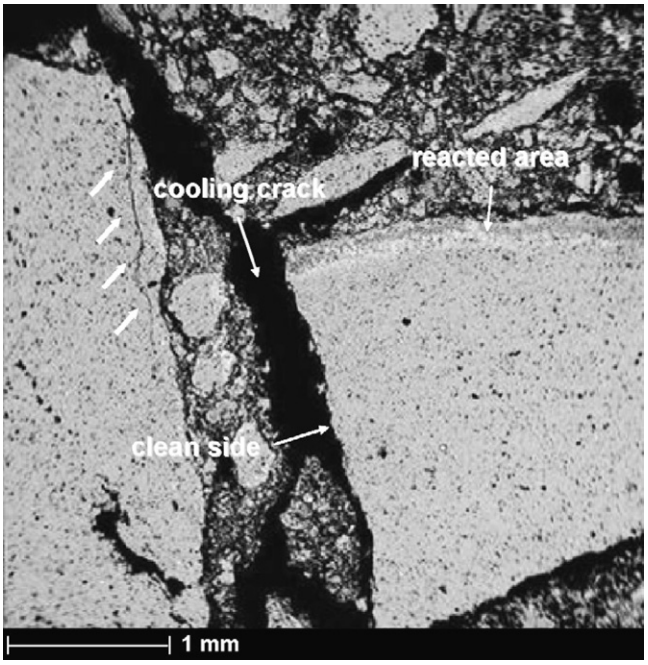

Fig. 11. Microstructure of M3 sample after firing at 1500 °C for 5 h, highlighting the cooling cracks [13].

the consequent stress around the MgO particle should also be higher, this is a clear reason for the higher overall expansion values. According to the results obtained by Braulio et al. [13] with the same M3 sample, the cracks identified in the SEM (Fig. 11) images were formed during the castable cooling step and, thus, could not be associated with the abnormal expansion detected in Fig. 10.

In order to solve this question, two additional aspects related to the spinel generation should be considered. The first one is related to the reaction mechanism proposed in Fig. 4 when two particles are in contact, which pointed out that the residual expansion depends on the volume of the generated pore (P) and on the expansion at the alumina side (ΔX). For the castables evaluated in this work, the porosity share on expansion should not be different, as the same amount of MgO was used. However, according to Nakagawa et al. [7], when dealing with multi-particles systems, such as refractory castables, ΔX can be significantly affected by the type and number of particle contacts.

In a powder compact comprising alumina and magnesia, three contact pairs are found: MgO–MgO, Al_2O_3–MgO and Al_2O_3–Al_2O_3. The former does not add to the ΔX value, as it shrinks, leading to the Kirkendall porosity, and, therefore, its effect is accounted in P. On the other hand, the Al_2O_3–MgO and Al_2O_3–Al_2O_3 pairs present positive volume change and their share on expansion depends on the thickness ratio, R. Table 3 presents the three types of contacts and their impact on the final expansion considering two R values, calculated by Nakagawa [7].

Table 3
The different types of contacts in an alumina–magnesia mixture and their contribution to the overall expansion considering $R = 3$ and $R = \infty$ [7].

Type of contact	ΔX increment (%)	
	$R = 3$	$R = \infty$
MgO–MgO	0	0
Al_2O_3–MgO	2.7	4.0
Al_2O_3–Al_2O_3	5.3	15.9

The increment for the Al_2O_3–MgO couple is lower than the Al_2O_3–Al_2O_3 one, due to the balanced effect between the alumina expansion and the magnesia shrinkage. Therefore, in a compact powder, the higher the number of Al_2O_3–Al_2O_3 contacts, the greater the ΔX value. Aiming to verify this aspect, the number of magnesia and alumina particles was estimated for the M1, M2 and M3 samples, considering the proportion of components used (dead-burnt magnesia, reactive alumina and fine tabular alumina < 200 μm) and their average diameter size. It was also assumed that the particles presented a spherical shape. These results are presented in Table 4, as the A/M ratio, which represents the number of alumina particles for each magnesia one in the mixture.

Increasing the magnesia grain size reduced the number of MgO particles added to the mixture and also the likelihood of a MgO–MgO contact, leading, therefore, to a high A/M ratio for the sample containing coarse magnesia (M3). Consequently, the number of Al_2O_3–MgO pairs is much higher in M1, whereas the contact Al_2O_3–Al_2O_3 should be predominant in M3. The Al_2O_3–Al_2O_3 pair counts with the largest portion of ΔX, mainly for high R value (as shown in Table 3), which partially explains the different expansive behavior observed in Fig. 8.

Additionally, as the spinel reaction is not the only mechanism taking place with the temperature, one should also consider the shrinkage related to the castable sintering. In Fig. 8, it can be observed that due to the higher reactivity of the magnesia grains and the close number of alumina and magnesia particles in the castable matrix (Table 4), the spinel formation started earlier in the M1 sample. Consequently, the reaction also finished at lower temperatures and a small sintering shrinkage could be detected between the spinel and the CA_6 peaks. This aspect is better highlighted in Fig. 12, which shows the derivative of the curves presented in Fig. 10 [25]. For the other two samples, part of the spinel formation occurred when CA_6 was already being generated. No shrinkage was then identified in the M2 and M3 curves.

Besides this, the different sintering profiles could also affect the expansion associated with the CA_6 formation. The CA_6 peak in the thermal expansion curves is the result of a balanced effect between the CA_6 expansion and the sintering shrinkage.

Table 4
A/M ratio of the castables M1 (MgO < 13 μm), M2 (MgO < 45 μm) and M3 (MgO < 100 μm).

	M1	M2	M3
A/M	∼5	∼100	∼5000

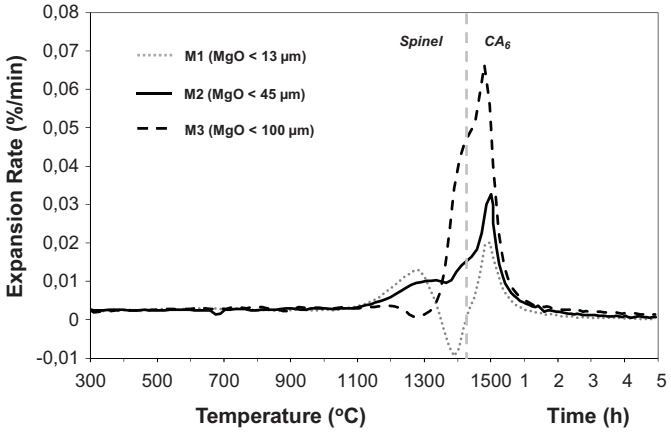

Fig. 12. Expansion rate of alumina–magnesia castables containing MgO of different grain sizes [25].

Therefore, the faster the spinel formation is the higher the sintering efficiency and the lower the CA_6 expansive effect. The micrographs present in Fig. 9 highlight the higher structure densification when using smaller MgO grains.

3.3. If the in situ spinel formation is followed by expansion and pore generation, why do spinel-forming castables usually present excellent corrosion resistance in industrial applications?

The spinel intrinsic expansion, regardless of the thickness ratio value (R) and the Kirkendall effect, should decrease the slag resistance of spinel-forming castables. However, Fig. 13(a) shows the results of corrosion tests using a high-iron oxide containing slag (∼45 wt%) carried out in the castable designed by adding MgO of intermediate grain size (M2), pointing out the high corrosion and infiltration resistance of this composition.

According to Sako et al. [19], although the *in situ* spinel formation indeed led to higher open porosity, the physical aspects were less important than the chemical interactions with the molten slag. For spinel-forming castable, as CA_6 formation involves the precipitation of CM_2A_8 ($CaMg_2Al_{16}O_{27}$) as a precursor phase, its microstructural configuration was associated with the previous location of the MgO sources. Thus, the CA_6 crystals generated during pre-firing at 1500 °C were spread all over the microstructure, including at the edges of coarse tabular alumina aggregates, which helped to chemically protect the material from further penetration.

Nevertheless, it is important to highlight that the above-mentioned conclusions were for the spinel-forming castable containing MgO of intermediate grain size (<45 μm). The results of the corrosion experiment for the M3 composition (MgO < 100 μm) showed higher penetration and wear rates (Fig. 13(b)). In this case, the *in situ* CA_6 generation was most likely carried out similar to the M2 sample. However, the excessive expansion during heating observed in Fig. 10 drastically affected the castable's physical properties and, consequently, had a negative effect on the corrosion resistance of the spinel-forming castable when using a high-iron oxide

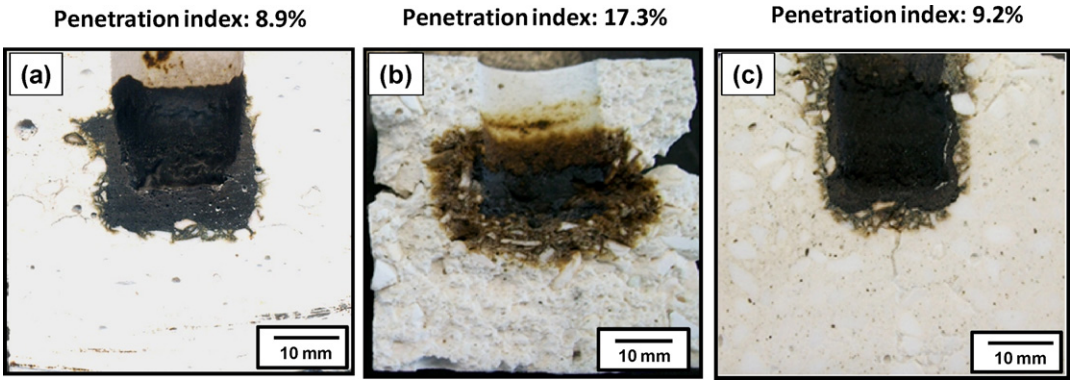

Fig. 13. Cross-sections and penetration indexes of alumina–magnesia castables after the corrosion tests at 1500 °C for 2 h. A high-iron oxide containing slag was used. (a) M2 (MgO < 45 μm); (b) M3 (MgO < 100 μm); and (c) M3 (MgO < 100 μm) under constraint.

containing slag. In fact, in the same test conducted under constraint, preventing the microstructure expansion and simulating an industrial application, the result was an increased slag resistance, as shown in Fig. 13(c).

Fig. 14 (a) presents the apparent porosity of the three castables (M1, M2 and M3) after firing at 1500 °C for 5 h at the two different conditions: free to expand and under constraint. The results pointed out that, when the sample was constrained, the high expansion of M3 led to a reduction of the apparent porosity and, consequently, of the slag penetration index, for the tests conducted in the same conditions (Fig. 14(b)).

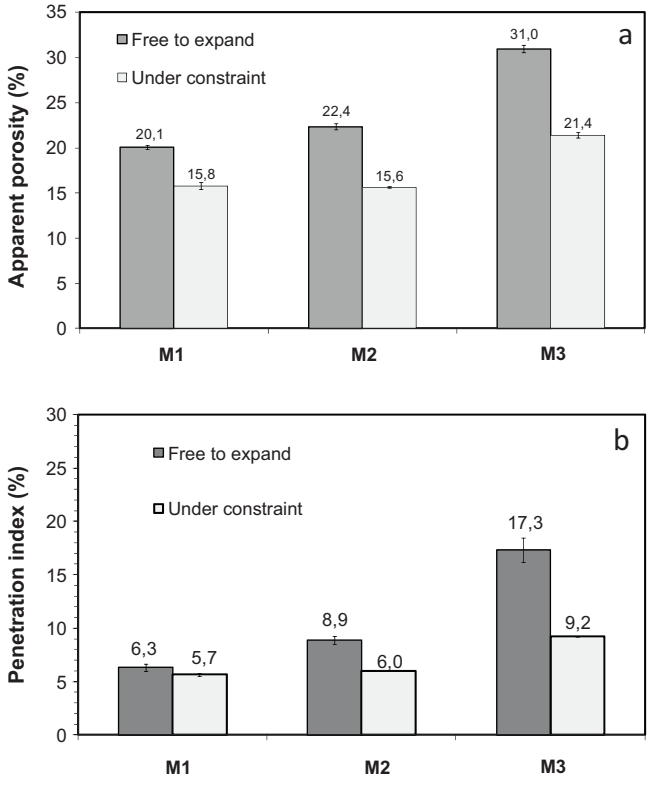

Fig. 14. Apparent porosity (a) and penetration index (b) of the castables M1 (MgO < 13 μm), M2 (MgO < 45 μm) and M3 (MgO <100 μm) after firing/corrosion experiment at 1500 °C for 5 h at two conditions: free to expand and under constraint.

The same behavior was observed for M1 and M2, but to a lesser extent. The results indicated that the excellent corrosion behavior of alumina–magnesia castables in industrial applications is associated with the structural constraint imposed by the surrounding lining materials, which reduces the drawbacks related to the expansive *in situ* spinel formation.

4. Conclusions

Based on the three proposed questions related to cement-bonded refractory castables, the main remarks of the present work can be summarized as follows:

- The faster Mg^{2+} mobility and the likelihood of reactions with a higher thickness ratio seem to induce the Kirkendall effect during the *in situ* spinel formation. Measurements based on SEM images indicated that the average pore size of the sample containing MgO < 45 μm (M2) increased with the firing temperature. In addition, a relationship between the pore size after firing at 1500 °C and the magnesia grain size was also detected, suggesting that the Kirkendall effect is the most likely reason for the spinel reaction being followed by pore generation.
- The different values of overall expansion observed in alumina–magnesia castables containing MgO of distinct grain sizes were not associated with the Kirkendall porosity, as the total volume of generated pores should be the same regardless of the MgO source. The permanent volumetric change scaled with the MgO grain size due to the increase in the number of Al_2O_3–Al_2O_3 pairs and reduced likelihood of a MgO–MgO contact. As these aspects depend on the largest portion of the spinel expansion, castables containing coarser MgO grains presented higher expansion. Additionally, the reaction for spinel formation was faster in samples containing smaller MgO grains, owing to the higher particles reactivity and close number of alumina–magnesia contacts. Consequently, the sintering efficiency was increased, reducing the overall expansion values.
- Regarding the corrosion resistance, besides the proper CA_6 crystals distribution through the microstructure, alumina–magnesia castables usually perform well in industrial

applications due to the benefits provided by the structural constraint. When preventing the castable expansion, even the compositions containing coarse MgO grains (M3) showed a suitable corrosion and penetration resistance, as a result of the reduced open porosity values.

Acknowledgements

The authors are grateful to the Federation for International Refractories Research and Education (FIRE) and the Brazilian funding agency CNPq for supporting this work.

References

[1] C. Wagner, The mechanism of formation of ionic compounds of higher order (Double salts, spinel, silicates), Zeitschrift Fur Physikalische Chemie B34 (1936) 209–316.
[2] R.E. Carter, Mechanism of solid-state reaction between magnesium oxide and aluminum oxide and between magnesium oxide and ferric oxide, Journal of the American Ceramic Society 44 (3) (1961) 116–120.
[3] L. Navias, Preparation and properties of spinel made by vapor transport and diffusion in the system $MgO–Al_2O_3$, Journal of the American Ceramic Society 44 (9) (1961) 434–446.
[4] R.C. Rossi, R.M. Fulrath, Epitaxial growth of spinel by reaction in the solid state, Journal of the American Ceramic Society 46 (3) (1963) 145–149.
[5] Z. Nakagawa, N. Enomoto, I. Yi, K. Asano, Effect of corundum/periclase sizes on expansion behavior during synthesis of spinel, in: Proceedings of UNITECR, Kyoto, Japan, (1995), pp. 379–386.
[6] Y. Kiyota, Reduction of permanent linear change of $Al_2O_3–MgO$ castable, in: Proceedings of UNITECR, Dresden, Germany, (2007), pp. 546–549.
[7] Z. Nakagawa, Expansion behavior of powder compacts during spinel formation, Mass and Charge Transport in Ceramics (1996) 283–294.
[8] A.D Smigelskas, E.O. Kirkendall, Zinc diffusion in alpha brass, Transactions of the AIME 171 (1947) 130–142.
[9] H.J. Fan, M. Knez, R. Scholz, K. Nielsch, E. Pippel, D. Hesse, M. Zacharias, U.G. Sele, Monocrystalline spinel nanotube fabrication based on the Kirkendall effect, Nature Materials 5 (2006) 627–631.
[10] S. Gopalan, A.V. Virkar, Interdiffusion and Kirkendall effect in doped $BaTiO_3–BaZrO_3$ perovskites: effects of vacancy supersaturation, Journal of American Ceramic Society 82 (10) (1999) 2887–2899.
[11] H. Strandlund, H. Larsson, Prediction of Kirkendall shift and porosity in binary and ternary diffusion couples, Acta Materialia 52 (2004) 4695–4703.
[12] H.C. Yu, D.H. Yeon, A. van der Ven, K. Thorton, Substitutional diffusion and Kirkendall effect in binary crystalline solids containing discrete vacancy sources and sinks, Acta Materialia 55 (2007) 6690–6704.
[13] M.A.L. Braulio, L.R.M. Bittencourt, V.C. Pandolfelli, Magnesia grain size effect on in situ spinel refractory castables, Journal of European Ceramic Society 28 (2008) 2845–2852.
[14] A. Kitamura, K. Onizuka, K. Tanaka, Hydration characteristics of magnesia, Taikabutsu Overseas 16 (3) (1995) 3–11.
[15] G. Ervin Jr., Oxidation behavior of silicon carbide, Journal of the American Ceramic Society 41 (9) (1958) 347–352.
[16] M. Schnabel, A. Buhr, R. Exenberger, C. Rampitsch, Spinel: in situ versus preformed – clearing the myth, Refractories World Forum 2 (2) (2010) 87–93.
[17] Y.-C. Ko, Influence of the characteristics of spinels on the slag resistance of $Al_2O_3–MgO$ and $Al_2O_3–$spinel castables, Journal of American Ceramic Society 83 (9) (2000) 2333–2335.
[18] M.A.L. Braulio, A.P. Luz, A.G. Tomba Martinez, C. Liebske, V.C. Pandolfelli, Basic slag attack of spinel-containing refractory castables, Ceramics International 37 (6) (2011) 1935–1945.
[19] E.Y. Sako, M.A.L. Braulio, V.C. Pandolfelli, The corrosion and microstructure relationship for cement-bonded spinel refractory castables, Ceramics International, submitted for publication.
[20] E.Y. Sako, M.A.L. Braulio, P.O. Brant, V.C. Pandolfelli, The impact of pre-formed and in situ spinel formation on the physical properties of cement-bonded high-alumina refractory castables, Ceramics International 36 (2010) 2079–2085.
[21] S. Zhang, W.E. Lee, Spinel-containing refractories, in: S. Zhang, W.E. Lee (Eds.), Refractories Handbook, Marcel Dekker Inc., USA, 2004, pp. 215–257.
[22] J.M. Auvray, C. Gault, M. Huger, Evolution of elastic properties and microstructural changes versus temperature in bonding phases of alumina and alumina–magnesia refractory castables, Journal of European Ceramic Society 27 (2007) 3489–3496.
[23] M.A.L. Braulio, L.R.M. Bittencourt, J. Poirier, V.C. Pandolfelli, Microsilica effects on cement-bonded alumina–magnesia refractory castables, Journal of the Technical Association of Refractories 28 (3) (2008) 180–184.
[24] E.Y. Sako, M.A.L. Braulio, D.H. Milanez, P.O. Brant, V.C. Pandolfelli, Microsilica role in the CA_6 formation in cement-bonded spinel refractory castables, Journal of Materials Processing Technology 209 (2009) 5552–5557.
[25] M.A.L. Braulio, J.F. Castro, C. Pagliosa, L.R.M. Bittencourt, V.C. Pandolfelli, From macro to nanomagnesia: designing the in situ spinel formation, Journal of the American Ceramic Society 91 (9) (2008) 3090–3093.